Hyperfine Interact (2007) 174:55–64
DOI 10.1007/s10751-007-9564-x

Optical clock and ultracold collisions with trapped strontium atoms

T. Zelevinsky · M. M. Boyd · A. D. Ludlow · S. M. Foreman · S. Blatt · T. Ido · J. Ye

Published online: 19 June 2007

Abstract With microkelvin neutral strontium atoms confined in an optical lattice, we have achieved a fractional resolution of better than 5×10^{-15} on the ${}^1S_0 - {}^3P_0$ doubly forbidden ^{87}Sr clock transition at 698 nm. Measurements of the clock line shifts as a function of experimental parameters indicate that the fractional uncertainties due to systematic shifts could be reduced below 10^{-15}. The ultrahigh spectral resolution permitted resolving the nuclear spin states of the clock transition at small magnetic fields, leading to measurements of the ${}^3P_0$ magnetic moment and metastable lifetime. In addition, photoassociation spectroscopy was performed on the narrow ${}^1S_0 - {}^3P_1$ transition of ^{88}Sr, revealing the least-bound state, and showing promise for efficient optical tuning of the ground state scattering length and production of cold molecules.

Keywords Optical clock · Photoassociation · Optical lattice

1 Introduction

The two-electron nature of alkaline earth atoms such as strontium permits studies of narrow line physics based on the forbidden ${}^1S_0 - {}^3P_0$ and ${}^1S_0 - {}^3P_1$ transitions. The ${}^1S_0 - {}^3P_0$ ^{87}Sr line at 698 nm is especially attractive for an optical atomic clock, since its natural lifetime is as long as about 150 s. Using optically cooled ^{87}Sr atoms in a zero-Stark-shift one-dimensional optical lattice and a cavity-stabilized probe laser with a sub-Hz spectral width, we have achieved repeatable Fourier-limited linewidths below 2 Hz. This represents a fractional resolution of better than 5×10^{-15}. We have characterized the accuracy of the clock as a function of experimental parameters such

T. Zelevinsky (✉) · M. M. Boyd · A. D. Ludlow ·
S. M. Foreman · S. Blatt · T. Ido · J. Ye
JILA, University of Colorado, UCB 440, Boulder, CO 80309, USA
e-mail: tz@colorado.edu

as the optical lattice wavelength and intensity, probe laser intensity, atom density, and magnetic field.

The hertz level linewidths allowed us to resolve all hyperfine components of the clock transition (nuclear spin is $I = 9/2$ for ^{87}Sr), and measure the differential ground-excited g-factor that arises from hyperfine mixing of $^3P_0$ with $^3P_1$ and $^1P_1$. This measurement yielded an experimental determination of the $^3P_0$ lifetime.

We have also carried out narrow line photoassociation studies with ^{88}Sr near the $^1S_0 - ^3P_1$ dissociation limit. The 15 kHz natural width of the molecular line allowed observation of nine least-bound molecular states. The line shapes were sensitive to thermal effects even at 2 μK ultracold temperatures, as well as to zero-point shifts by the optical lattice confinement.

We showed that the combination of a narrow width of the least-bound state (at 0.4 MHz detuning) and its strong coupling to the scattering state should allow efficient tuning of the ground state scattering length with the optical Feshbach resonance technique. It is particularly important for ^{88}Sr, for example to enhance the elastic scattering rate, since the natural scattering length is close to zero, and there is no hyperfine structure to give rise to magnetic Feshbach resonances. We also predict that the deepest-bound level we observed decays to a single ground electronic molecular state with a high efficiency. This is promising for producing ultracold molecules through photoassociation, which is the subject of our ongoing and future research.

2 Optical atomic clock

Optical clocks based on neutral atoms tightly confined in optical lattices have recently begun to show promise as future frequency standards [1–4]. These optical lattice clocks enjoy a relatively high signal-to-noise ratio from the large numbers of atoms, while at the same time allowing Doppler-free interrogation of the clock transitions for long probing times, a feature typically associated with single trapped ions. Currently, detailed evaluations of systematic effects for the $^1S_0 - ^3P_0$ sub-Hz line in ^{87}Sr are being performed in several independent systems [1, 4, 5]. Here we present our recent progress toward evaluation of systematic effects at the 10^{-15} level. These measurements have greatly benefited from an ultranarrow spectral linewidth corresponding to a line quality factor $Q \sim 2.4 \times 10^{14}$ [6].

2.1 Experimental technique

Neutral strontium atoms are loaded into a dual-stage magneto-optical trap, where they are first cooled to mK temperatures using the strong (32 MHz) $^1S_0 - ^1P_1$ line, and then to μK temperatures using the weak (7 kHz) $^1S_0 - ^3P_1$ intercombination line [7]. Approximately 10^4 atoms at ~ 2 μK are loaded into a one-dimensional ~ 300 mW standing wave (optical lattice). The lattice wavelength of 813 nm is chosen to zero the net Stark shift of the clock transition [8], thus also eliminating line broadening due to the trapping potential inhomogeneity.

The atoms are confined in the Lamb–Dicke regime, such that the recoil frequency (5 kHz) is much smaller than the axial trapping frequency (50 kHz). As long as

the probe is carefully aligned along the lattice axis, spectroscopy is both first-order-Doppler-free and recoil-free. In the transverse direction, the lattice provides a trapping frequency of about 150 Hz, which is smaller than the recoil frequency, but still much larger than the clock transition linewidth. Atoms can be held in the perturbation-free lattice for times exceeding 1 s, which is important for hertz level spectroscopy.

We probe the extremely narrow clock transition in ^{87}Sr (natural width $\sim$ 1 mHz) with a cavity-stabilized diode laser operating at 698 nm. The high finesse cavity is mounted in a vertical orientation to reduce sensitivity to vibrations [9]. To characterize the probe laser, we compare it to a second stable laser locked to an identical cavity. This comparison shows laser linewidths below 0.2 Hz for a 5 s integration time (resolution bandwidth limited) and below 2.1 Hz for a 30 s integration time (limited by nonlinear laser drift).

For absolute frequency measurements of the clock transition, we frequency count the probe laser against a hydrogen maser microwave signal that is calibrated by the NIST primary Cs fountain clock. A self-referenced octave spanning frequency comb [10] is locked to the probe laser, while its repetition rate is counted against the maser. The fractional frequency instability of this counting signal is $2.5 \times 10^{-13}\ \tau^{-1/2}$ for an integration time τ, which is the primary limitation on our statistics.

2.2 Systematic effects

When the Zeeman sublevels of the ground and excited clock states are degenerate (nuclear spin $I = 9/2$), the linewidths of < 5 Hz ($Q \sim 10^{14}$) are achieved. This spectral resolution should allow us to push the fractional uncertainties of the measurements of systematic effects below 10^{-15}, limited by our microwave frequency reference.

The evaluation of systematic effects benefiting most directly from the high line Q is that of the frequency shift associated with an ambient magnetic field. The differential magnetic moment between the ground and excited states leads to a first-order Zeeman shift of the clock transition. This can lead to shifts or broadening from stray magnetic fields, depending on the population distribution among the magnetic sublevels. By varying the strength of an applied magnetic field in three orthogonal directions and measuring the spectral linewidth as a function of field strength, the uncertainty of the residual magnetic field has been reduced to < 5 mG for each axis. The resulting net uncertainty for magnetically-induced frequency shifts is now 0.6 Hz ($\sim 1 \times 10^{-15}$ fractionally). Understanding and controlling the magnetic shifts is essential for improvement of the ^{87}Sr frequency standard since the accuracy of all recent measurements has been limited by the sensitivity to magnetic fields [1, 2, 4].

Reduction of the other systematic uncertainties (due to lattice intensity, probe intensity, and atom density) is straightforward with our high spectral resolution, and is currently underway. Even when we stabilize the microwave phase of the fiber that transmits the reference from NIST to JILA to take full advantage of the accuracy of the microwave reference, the averaging times necessary to achieve 10^{-15} uncertainties for all systematic effects are still quite long. Our approach to most systematic effect measurements is thus to take interleaved line scans that sample several values of the same systematic parameter during the scan, and finding the linear slope. The results are to be reported in an upcoming publication. In addition,

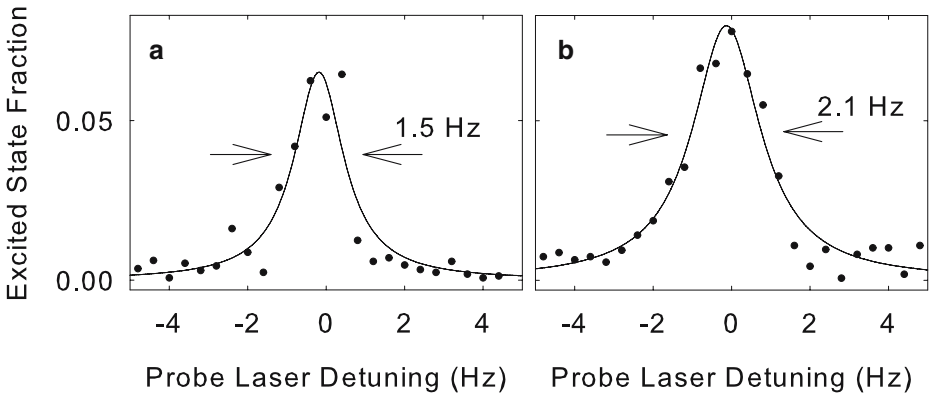

Fig. 1 Typical spectra of the ${}^1S_1 - {}^3P_0$ clock transition, exhibiting a line quality factor $Q \sim 2.4 \times 10^{14}$. The linewidths are **a** 1.5(2) Hz and **b** 2.1(2) Hz, in good agreement with the probe time limit of 1.8 Hz. One such trace takes approximately 30 s to collect (since the atom trap must be reloaded for each data point), and involves no averaging or normalization

we have locked the probe laser to the clock transition with the goal of directly comparing the Sr clock to the Ca and Hg^+ optical atomic clocks at NIST.

2.3 High spectral resolution

The recent improvements to the probe laser stabilization have allowed us to probe the clock transition at an unprecedented level of spectral resolution. With the nuclear spin degeneracy removed by a small magnetic field, individual transition components allow exploring the ultimate limit of our resolution by eliminating any broadening due to residual magnetic fields or light shifts. Figure 1 shows sample spectra of the ${}^1S_0(m_F = 5/2) - {}^3P_0(m_F = 5/2)$ transition, where m_F is the nuclear spin projection onto the lattice polarization axis. The linewidths are probe time limited to ~ 1.8 Hz, representing a line Q of $\sim 2.4 \times 10^{14}$. This Q value can be reproduced reliably, with some scatter of the measured linewidths in the $\sim 1 - 3$ Hz range.

Besides the single-pulse spectroscopy of the clock line, two-pulse optical Ramsey experiments were also performed on an isolated Zeeman component. When a system is limited by the atom or trap lifetime, the Ramsey technique can yield higher spectral resolution at the expense of fringe contrast, and generally for the same spectroscopy time, the resolution is slightly higher for the Ramsey case. An additional motivation for Ramsey spectroscopy in the Lamb–Dicke regime is the ability to use long interrogation pulses, which results in a drastically narrowed Rabi pedestal compared to what is typically seen for free-space atoms. The reduced number of Ramsey fringes facilitates the identification of the central fringe for applications such as frequency metrology.

Figure 2a shows a sample Ramsey spectrum, where the preparation and probe pulses are 20 ms and the free evolution time is 25 ms, yielding a pattern with a fringe width of 10.4(2) Hz, as expected. Figure 2b shows the same transition with the preparation and probe pulses of 80 ms and the evolution time of 200 ms. Here the width of the central fringe is reduced to 1.7(1) Hz. Both spectra exhibit no degradation of the fringe contrast. However, the quality of the spectra deteriorated

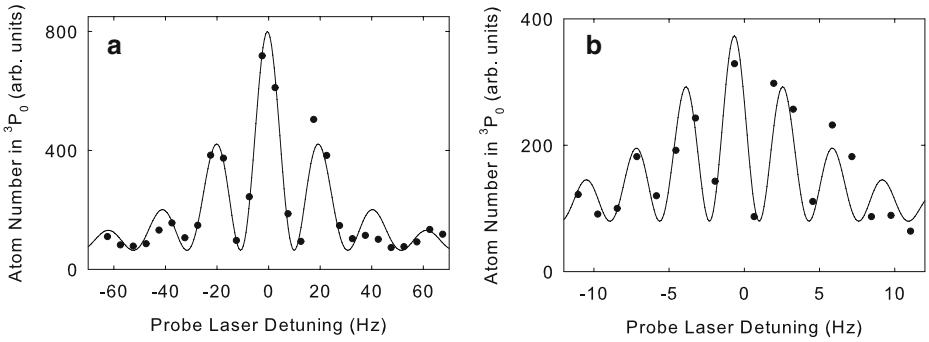

Fig. 2 Ramsey spectra of the $^1S_1 - ^3P_0$ clock transition. **a** The preparation and probe pulses are 20 ms, the evolution time is 25 ms. Fringe width is 10.4(2) Hz. **b** The preparation and probe pulses are 80 ms, the evolution time is 200 ms. Fringe width is 1.7(1) Hz

at longer evolution times. Our inability to increase the resolution as compared to single-pulse Rabi spectroscopy suggests that the linewidth is not limited by the atom or trap lifetime, but rather by phase decoherence between the light and atoms, most likely due to nonlinear laser frequency fluctuations during the scan. This is supported by single-pulse spectroscopy where the linewidth repeatability at the probe time limit near 0.9 Hz appeared limited by the laser stability.

2.4 Magnetic moment and lifetime measurements on the clock transition

This high spectral resolution allowed us to perform NMR-type experiments in the optical domain. We applied a small magnetic bias field and made direct observations of the magnetic sublevels associated with the nuclear spin. The magnetic moments of $^1S_0$ and $^3P_0$ differ because of hyperfine-induced state mixing of $^3P_0$ with $^3P_1$ and $^1P_1$. The differential Landé g-factor, Δg, leads to a ~ 110 Hz/(G m_F) linear Zeeman shift of the clock line. This Zeeman shift measurement is also a direct determination of the perturbed wavefunction of $^3P_0$, and hence of its metastable (~ 100 s) lifetime. Our approach uses only a small magnetic field, while traditional NMR experiments performed on either $^1S_0$ or $^3P_0$ would need large magnetic fields to induce splitting in the radio frequency range. As larger fields can give rise to additional field-induced state mixing between $^3P_0$, $^3P_1$, and $^1P_1$ (we estimate that a field as weak as 16 G causes a 1% change in Δg), the use of a small field permits an accurate, unperturbed measurement of mixing effects. Additionally, this measurement on the resolved transitions is helpful for the optical clock accuracy evaluation, as one can look for changes in the splitting as a function of the lattice polarization to measure the effect of polarization-dependent light shifts.

The differential nuclear magnetic moment can be determined by setting the probe light polarization parallel to the lattice polarization axis and magnetic field direction, and fitting the resulting Zeeman splitting of the π-transitions. However, such a measurement requires an independent calibration of the magnetic field in the trap region, and is sensitive to the linear drift of the probe laser during the scan, which manifests as a fictitious magnetic field. In a more powerful measurement scheme, we instead polarize the probe laser perpendicular to the quantum axis to excite σ^+

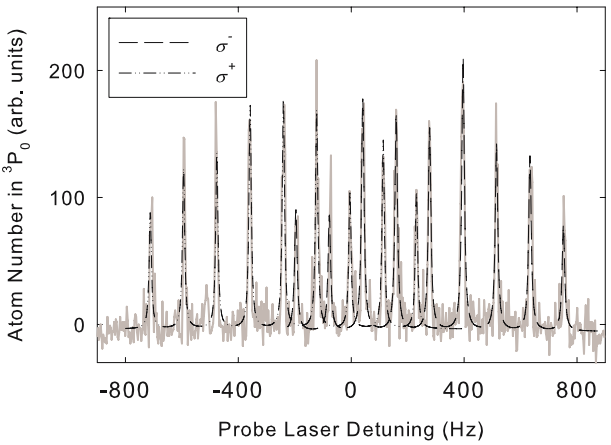

Fig. 3 Clock transition with resolved nuclear spin sublevels. The probe light is polarized perpendicular to the magnetic field direction and lattice polarization, in order to probe σ transitions. The σ^+ and σ^- components are seen as two combs with nine individual lines (nuclear spin $I = 9/2$). The spacing between these lines is determined by the differential g-factor of the two clock states, Δg

and σ^- transitions, to obtain spectra as in Fig. 3. Each spectrum yields information about the Δg value from the splitting between the neighboring σ^+ or σ^- lines, and about the magnetic field from the splitting between the two manifolds, since the ground state magnetic moment is well known [11]. Thus the nuclear spin is used as a magnetometer. Since the field calibration and the Δg measurement are done simultaneously, this approach is immune to any linear laser drift or magnetic field variation. This method also eliminates a Δg sign ambiguity that is present in the π-transition approach.

We found that the linear Zeeman shift of the clock transition is $-108.4(4)$ Hz m_F/G, corresponding to a $^3P_0$ magnetic moment of $-1.732(7)\mu_N$, where μ_N is the nuclear magneton. To check for systematic errors related to light shifts, we varied the intensities of the lattice laser (by $> 50\%$) and the probe laser (by a factor of 10) and observed no statistically significant change in the measured splitting. We have also searched for possible m_F-dependent systematics by comparing the splitting frequency of different pairs of sublevels. The magnetic field was varied to verify the field independence of the measurement.

A combination of our Δg measurements with atomic theory of hyperfine mixing [12, 13] can predict the metastable lifetime of $^3P_0$. Depending on the specifics of the chosen model, the predicted lifetimes range between 100 and 180 seconds. Although our experimental measurement error is small, it results in a relatively large model-dependent error associated with the lifetime measurement, which gives the value of 140(40) s. Still it is a very useful confirmation of recently calculated values, since a direct and accurate measurement of the natural lifetime is difficult due to limitations from the trap lifetime and blackbody quenching.

3 Narrow line photoassociation

While we worked with the doubly forbidden transition of ^{87}Sr in the optical clock experiments, we used ^{88}Sr for cold collision studies. The even isotope is the most abundant (83%), and has a zero nuclear spin. The large abundance helps keep the sample denser in the trap for more efficient collisions, and the absence of the nuclear

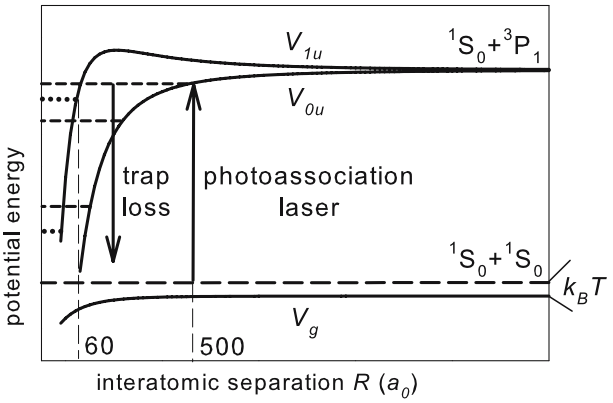

Fig. 4 Schematic diagram of the long-range Sr_2 molecular potentials. At large internuclear separations, the ground and excited molecular states correspond to two ground state atoms, and to one ground and one excited state atom, respectively. The ground state has *gerade* symmetry and its energy is given by the potential V_g, while the excited state *ungerade* potentials that support transitions to the ground state are V_{0u} and V_{1u}, the latter with a small repulsive barrier. All vibrational states of 0_u and 1_u (*dashed* and *dotted lines*, respectively) are separated by more than the natural line width, permitting high resolution PA spectroscopy very close to the dissociation limit when the atoms are sufficiently cold

spin greatly simplifies the molecular potentials, thus facilitating comparisons of experiment and theory. With ultracold ^{88}Sr in a zero-Stark-shift optical lattice (914 nm wavelength), we performed narrow line photoassociation (PA) spectroscopy near the $^1S_0 - ^3P_1$ intercombination transition [14]. Nine least-bound vibrational molecular levels associated with the long-range 0_u and 1_u excited molecular potentials were measured and identified. The measured PA resonance strengths showed that optical tuning of the ground state scattering length should be possible without significant atom loss. The calculated decay strengths of the photoassociated molecules to the ground electronic state indicate great promise for ultracold stable molecule production.

In contrast to prior PA work that utilizes strongly allowed transitions with typical line widths in the MHz range, here the spin-forbidden atomic $^1S_0 - ^3P_1$ line has a natural width of ~ 7 kHz. This narrow width allows us to measure the least-bound vibrational levels that would otherwise be obscured by a broad atomic line, and to observe characteristic thermal line shapes even at μK atom temperatures. It also permits examination of the unique crossover regime between the van der Waals and resonant dipole-dipole interactions, that occurs here very close to the dissociation limit. This access to the van der Waals interactions ensures large bound–bound Franck–Condon factors, and may lead to more efficient creation of cold ground state Sr_2 molecules with two-color PA than what is possible using broad transitions.

Figure 4 illustrates the relevant potential energy curves for the Sr_2 dimer as a function of interatomic separation R. The photoassociation laser induces allowed transitions from the separated $^1S_0$ atom continuum at the temperature $T \sim 2$ μK to the bound vibrational levels of the excited potentials V_{0u} and V_{1u}, corresponding to the total atomic angular momentum projections onto the internuclear axis of 0 and 1, respectively. The long-range potentials are determined by the C_6/R^6 (van der

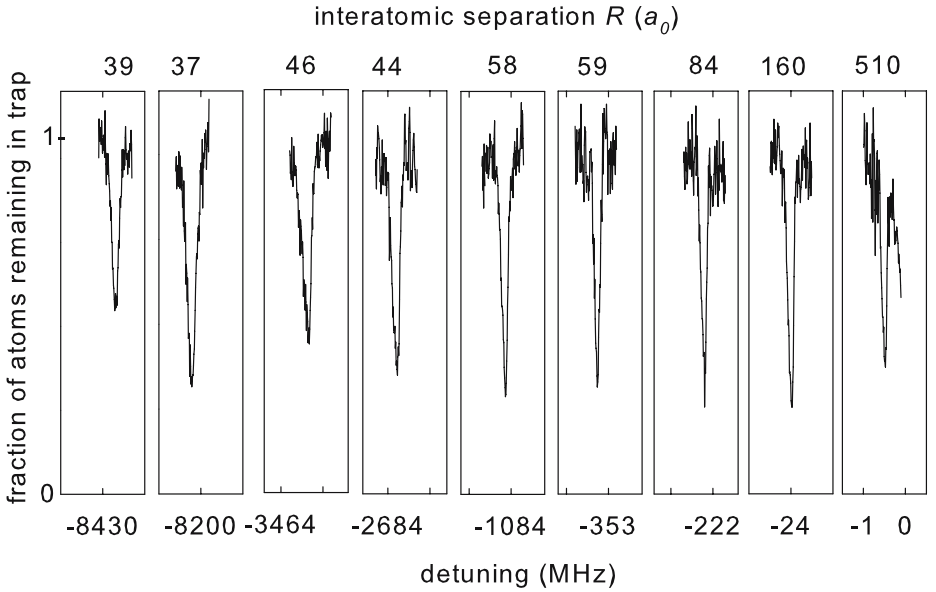

Fig. 5 The spectrum of the long-range Sr_2 molecule near the $^1S_0 - ^3P_1$ dissociation limit. The *horizontal scale* is marked on the *rightmost panel* and is the same for each of the nine blocks; different PA laser intensities were used for each line due to largely varying transition strengths. The top labels indicate the interatomic separations that correspond to the classical outer turning points of each resonance. The least-bound (−0.4 MHz) state has a very strong coupling to the scattering state, and could be used to control ultracold collisions. The deepest (−8.4 GHz) of these bound states has a ~ 0.9 Franck–Condon coupling coefficient to the ground molecular state, and could be used for cold molecule production

Waals) and C_3/R^3 (resonant dipole-dipole) interactions. The values of the C_3 and C_6 coefficients are adjusted in the multi-channel theoretical model [15] so that bound states exist at the experimentally determined resonance energies. The C_3 coefficient can be expressed in terms of the atomic lifetime τ as $C_3 = 3\hbar c^3/(4\tau\omega^3)$, where $\hbar\omega$ is the atomic transition energy and c is the speed of light. Our data and theoretical model yielded a C_3 coefficient that corresponds to the $^3P_1$ atomic lifetime of 21.5(2) μs.

To trace out the molecular line spectra, a 689 nm diode laser is frequency stabilized and tuned near the $^1S_0 - ^3P_1$ intercombination line. The laser frequency is stepped, and after 320 ms of photoassociation at a fixed frequency the atoms are released from the optical lattice trap and illuminated with a strongly resonant light pulse for atom counting. At a PA resonance, the atom number drops as excited molecules form and subsequently decay to ground state molecules in high vibrational states or hot atoms that cannot remain trapped. Figure 5 shows the nine observed PA line spectra near the dissociation limit. The individual lines were fit to convolutions of a Lorentzian profile with an initial thermal distribution, and distinct thermal tails were observed even at the ultracold $\sim 1-3$ μK temperatures. In addition, the strong axial lattice confinement alters the collisional dynamics, and the two dimensional effects factor into the lineshapes as a larger density of states at small thermal energies, and as a red shift by the lattice zero-point confinement frequency.

Intercombination transitions of alkaline earths such as Sr are particularly good candidates for optical control of the ground state scattering length, $a + a_{\rm opt}$, because there is a possibility of large gains in $a_{\rm opt}$ with small atom losses. These optical Feshbach resonances are of great interest for Sr, since magnetic Feshbach resonances are absent for the $^1S_0$ ground state, and the background scattering length is too small to allow evaporative cooling [16]. Using the -0.4 MHz PA line (see Fig. 5) should allow tuning the ground state scattering length [17] by $\pm 300\, a_0$ (a_0 is the Bohr radius), where the PA laser with intensity $I = 10$ W/cm^2 is far-detuned by $\delta = \pm 160$ MHz from the molecular resonance. In contrast, optical tuning of the scattering length in alkali ^{87}Rb [18] achieved tuning of $\pm 90\, a_0$ at much larger PA laser intensities of 500 W/cm^2. In addition, the Sr system at the given parameter values will have a loss rate of [17] $\sim 2 \times 10^{-14}$ cm^3/s, while the loss rate in the ^{87}Rb experiment was 2×10^{-10} cm^3/s. The overall efficiency gain of over 5 orders of magnitude is possible for Sr because the narrow intercombination transition allows access to the least-bound molecular state, and the PA line strength exponentially increases with decreasing detuning from the atomic resonance [17]. The above scattering length tunings and atom loss values accessible with the -0.4 MHz resonance result in the elastic and inelastic collision rates of $\Gamma_{\rm el} \sim 600$/s and $\Gamma_{\rm inel} \sim 0.1$/s, respectively. The favorable $\Gamma_{\rm el}/\Gamma_{\rm inel}$ ratio may enable evaporative cooling. However, a stringent constraint on the use of narrow-line optical Feshbach resonances is the proximity of the atomic transition. Here, the scattering rate of the PA laser photons due to the $^1S_0 - ^3P_1$ atomic line is $\Gamma_s \sim 40$/s $\sim \Gamma_{\rm el}/15$. Excessive one-atom photon scattering can cause heating and loss of atoms from the lattice.

Another potential application of narrow line PA is efficient production of ultracold molecules in the ground electronic state. Because the Sr excited state molecular potential is strongly influenced by van der Waals (C_6) interactions, the wavefunction overlap with the ground molecular bound states is large, and it might be possible to use low-power lasers in a Raman configuration to coherently transfer the molecules into the absolute ground ro-vibrational molecular state. Other exciting prospects include using the Raman scheme to perform precision measurements of the molecular ground state vibrational spacings with the goal of constraining temporal variations of the proton-electron mass ratio, and combining strontium with other alkaline earth atoms to create strongly interacting ultracold polar molecules in an optical lattice.

Acknowledgements We thank S. Diddams, T. Parker and L. Hollberg for facilitating the maser transfer from NIST and M. Notcutt and J. Hall for help with the probe laser. We also acknowledge theory collaboration with R. Ciuryło, P. Naidon and P. Julienne, and funding by NSF, NIST and ONR.

References

1. Ludlow, A., et al.: Systematic study of the ^{87}Sr clock transition in an optical lattice. Phys. Rev. Lett. **96**, 033003 (2006)
2. Takamoto, M., et al.: An optical lattice clock. Nature **435**, 321 (2005)
3. Barber, Z., et al.: Direct excitation of the forbidden clock transition in neutral ^{174}Yb atoms confined in an optical lattice. Phys. Rev. Lett. **96**, 083002 (2006)
4. Le Targat, R., et al.: Accurate optical lattice clock with ^{87}Sr atoms. Phys. Rev. Lett. **97**, 130801 (2006)
5. Takamoto, M., et al.: Improved frequency measurement of a one-dimensional optical lattice clock with a spin-polarized fermionic ^{87}Sr isotope. J. Phys. Soc. Japan **75**, 10 (2006)

6. Boyd, M., et al.: Optical atomic coherence at the 1-second time scale. Science **314**, 1430 (2006)
7. Loftus, T., et al.: Narrow line cooling and momentum-space crystals. Phys. Rev. A **70**, 063413 (2004)
8. Ido, T., Katori, H.: Narrow line cooling: finite photon recoil dynamics. Phys. Rev. Lett. **91**, 053001 (2003)
9. Notcutt, M., et al.: Simple and compact 1-Hz laser system via an improved mounting configuration of a reference cavity. Opt. Lett. **30**, 1815 (2005)
10. Fortier, T., et al.: Phase stabilization of an octave-spanning Ti: sapphire laser. Opt. Lett. **28**, 2198 (2003)
11. Olschewski, L.: Zeitschrift für Physik **249**, 205 (1972)
12. Kluge, H., Sauter, H.: Zeitschrift für Physik **270**, 295 (1974)
13. Lahaye, B., Margerie, J.: J. Phys. **36**, 943 (1975)
14. Zelevinsky, T., et al.: Narrow line photoassociation in an optical lattice. Phys. Rev. Lett. **96**, 203201 (2006)
15. Ciuryło, R., et al.: Photoassociation spectroscopy of cold alkaline-earth-metal atoms near the intercombination line. Phys. Rev. A **70**, 062710 (2004)
16. Mickelson, P., et al.: Spectroscopic determination of the *s*-wave scattering lengths of ^{86}Sr and ^{88}Sr. Phys. Rev. Lett. **95**, 223002 (2005)
17. Ciuryło, R., et al.: Optical tuning of the scattering length of cold alkaline-earth-metal atoms. Phys. Rev. A **71**, 030701(R) (2005)
18. Theis, M., et al.: Tuning the scattering length with an optically induced Feshbach resonance. Phys. Rev. Lett. **93**, 123001 (2004)